Photodissociation of CH2I2 and Subsequent Electron Transfer in Solution

4 AUTHORS, INCLUDING:

Ken-Ichi Saitow
Hiroshima University

54 PUBLICATIONS **771** CITATIONS

SEE PROFILE

Keitaro Yoshihara
The Graduate University for Advanced Stud…

302 PUBLICATIONS **7,973** CITATIONS

SEE PROFILE

FULL PAPERS

Photodissociation of CH₂I₂ and Subsequent Electron Transfer in Solution

Ken-ichi Saitow,*[a] Yukito Naitoh,[b] Keisuke Tominaga,[a, b] and Keitaro Yoshihara*[a, b]

Abstract: We studied photoinduced reactions of diiodomethane (CH_2I_2) upon excitation at 268 nm in acetonitrile and hexane by subpicosecond–nanosecond transient absorption spectroscopy. The transient spectra involve two absorption bands centered at around 400 (intense) and 540 nm (weak). The transients probed over the range 340–740 nm show common time profiles consisting of a fast rise (< 200 fs), a fast decay (≈ 500 fs), and a slow rise. The two fast components were independent of solute concentration, whereas the slow rise became faster (7–50 ps) when the concentration in both solutions was increased. We assigned the fast components to the generation of a CH_2I radical by direct dissociation of the photoexcited CH_2I_2 and its disappearance by subsequent primary geminate recombination. The concentration-dependent slow rise produced the absorption bands centered at 400 and 540 nm. The former consists of different time-dependent bands at 385 and 430 nm. The band near 430 nm grew first and was assigned to a charge-transfer (CT) complex, $CH_2I_2^{\delta+}\cdots I^{\delta-}$, formed by a photofragment I atom and the solute CH_2I_2 molecule. The CT complex is followed by full electron transfer, which then develops the band of the ion pair $CH_2I_2^{+}\cdots I^{-}$ at 385 nm on the picosecond timescale. On the nanosecond scale, I_3^{-} was generated after decay of the ion pair. The reaction scheme and kinetics were elucidated by the time-resolved absorption spectra and the reaction rate equations. We ascribed concentration-dependent dynamics to the CT-complex formation in pre-existing aggregates of CH_2I_2 and analyzed how solutes are aggregated at a given bulk concentration by evaluating a relative local concentration. Whereas the local concentration in hexane monotonically increased as a function of the bulk concentration, that in acetonitrile gradually became saturated. The number of CH_2I_2 molecules that can participate in CT-complex formation has an upper limit that depends on the size of aggregation or spatial restriction in the neighboring region of the initially photoexcited CH_2I_2. Such conditions were achieved at lower concentrations in acetonitrile than in hexane.

Introduction

Photochemical reactions in the condensed phase, in comparison with those in the gas phase, often give different kinetics and dynamics owing to continual interactions with solvent molecules.[1–4] In the case of photodissociation, solvent caging causes geminate recombination between photofragments[5–8] and further induces a secondary reaction between

[a] Prof. Dr. K.-i. Saitow,+ Prof. Dr. K. Tominaga,+++
Prof. Dr. K. Yoshihara++++
The Graduate University for Advanced Studies
Myodaiji, Okazaki 444-8585 (Japan)
E-mail: saitow@hiroshima-u.ac.jp
        riken-yoshihara@mosk.tytlabs.co.jp

[b] Dr. Y. Naitoh,++ Prof. Dr. K. Tominaga,+++ Prof. Dr. K. Yoshihara++++
Institute for Molecular Science
Myodaiji, Okazaki 444-8585 (Japan)

[+] Present address: Natural Science Center for Basic Research and
Development (N-BARD)
Hiroshima University
Kagamiyama, Higashi-Hiroshima 739-8526 (Japan)
Fax: (+81)82-424-7487
and

Department of Chemistry
Graduate School of Science
Hiroshima University
Kagamiyama, Higashi-Hiroshima 739-8526 (Japan)
and
PRESTO, JST, 4-1-8, Honcho Kawaguchi
Saitama 332-0012 (Japan)

[++] National Institute of Information and Communications Technology
588-2 Iwaoka, Iwaoka-cho, Kobe 651-2492 (Japan)

[+++] Molecular Photoscience Research Center
Kobe University, Nada, Kobe 657-8501 (Japan)
and
CREST, JST, Nada, Kobe 657-8501 (Japan)

[++++] Toyota Physical and Chemical Research Institute
Nagakute, Aichi 480-1192 (Japan)
Fax: (+81)561-63-6302

the photofragment and solute or solvent molecules.[9–14] A small simple molecule as a reactant could provide an advantage for evaluating microscopic details of solute–solvent interactions by minimizing interference from competing intramolecular pathways.[5–18] Alkyl halides show characteristic photochemical reactions in the condensed phase, which offer different photoproducts in contrast to that in the gas phase. Photolyzed halogen fragments are well-known as activated atoms to form charge–transfer (CT) complexes with solvent or solute molecules[9–12] or to give other products by hydrogen abstraction[13] or electron-transfer reactions.[14]

Polyhalomethanes in the condensed phase are typical examples of the alkyl halides mentioned above, and many reaction pathways and assignments of products have been reported over the last 40 years.[19–44] Neat CCl_4 was most extensively studied, and transient absorption bands at around 335 and 500 nm were commonly observed by the excitation sources of ultraviolet, pulsed-electron beam, and γ-ray.[19–25] These bands were assigned to various products, that is, CCl_2,[19] CCl_4^+,[20] CCl_3^+,[21] solvent-separated $CCl_3^+Cl^-$,[22,23] and ion-pair complex $CCl_4^+\cdots Cl^-$.[24] Through a subnanosecond transient absorption experiment and ab initio calculations, Bühler assigned the UV and visible bands to CCl_4^+ and the CT complex of CCl_3^+, respectively.[25]

For the photolysis of halomethanes in low-temperature matrices, it is known that UV irradiation gives a transient product as a "color center", which causes an intense and broad absorption band in the UV/Vis region. As for polyhalomethanes in a 3-methylpentane (3MP) matrix, Simons and co-workers found a color center upon UV irradiation.[26a,b] They assigned it to a trapped electron and suggested the characteristic reaction for its formation in contrast to their studies in the gas phase.[26c,d] They also observed generation of trihalide ions, for example, I_3^-, by warming the colored matrices.[26b] These characteristic reactions were ascribed to the photoexcitation of a polyhalomethane cluster in matrices.

Many investigators studied diiodomethane (CH_2I_2) and reported absorption spectra of transient products in low-temperature matrices by UV[26a,b,27a,28] and VUV[29] irradiations. UV irradiation at around 300 nm in 3MP matrix produced broad absorption bands at around 385 (intense) and 570 nm (weak). The former was assigned to $CH_2I_2^+$.[27a] The absorption intensity showed a sublinear concentration dependence, which suggests interaction of solutes in forming $CH_2I_2^+$. The band at 370 nm in an Ar matrix was identified as $CH_2I_2^+$ by photoelectron spectroscopy.[29]

Another assignment for this broad absorption band at around 370 nm was proposed to be an isomerization to $CH_2–I–I$ as a result of difference absorption spectra in the IR region and ab initio calculations.[28] Bond formation between the halogen of the $CH_2–I$ radical and the I radical after photodissociation was suggested as a reaction mechanism.

For reference, we briefly introduce the well-defined studies of photoexcited CH_2I_2 in the gas phase.[45–56] The UV absorption band, which lies between 200 and 350 nm, is as-
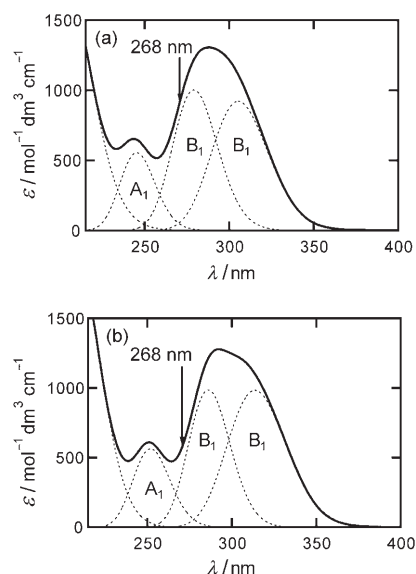

Figure 1. Static absorption spectra of CH_2I_2 in a) acetonitrile and b) hexane. Spectra are deconvoluted into a sum of four Gaussian bands (dashed lines). These bands are assigned to the electronic excited B_1, B_1, and A_1 states.[46] Arrows indicate the excitation wavelength used in the femtosecond transient absorption measurements.

signed to four or five n→σ* transitions[45–49] (Figure 1). UV excitation (<5 eV) induces photodissociation to the CH_2I radical and I atom. A flash photolysis experiment showed generation of the CH_2I radical, the ground state I ($^2P_{3/2}$), and the spin–orbit excited state I* ($^2P_{1/2}$) fragments.[45] Opto-acoustic[46] and IR emission[47] experiments showed that the excitation of the first B_1 band is correlated with production of only I, whereas the excitation of the second B_1 band is correlated with both I and I*. The branching ratios I*/I were reported to be 0 upon excitation to the first B_1, 0.57 to the second B_1, and 0.91 to the A_1 states.[46] Anisotropic parameters of fragments upon excitation at 310[49], 266,[50] and 304 nm[51] revealed that the photoexcited CH_2I_2 causes direct dissociation, and the dissociation process is very fast. The lifetime of the first dissociative state of CH_2I_2 was theoretically calculated to be very short (<80[54] and <8 fs[55]) owing to the direct dissociation.

Femtosecond time-resolved investigations of CH_2I_2 in solution at room temperature have been conducted by several researchers since 1993.[34–38] Schwarts et al. observed the ultrafast formation of CH_2I radical at 620 nm by the photodissociation of CH_2I_2 upon excitation of the B_1 state at 310 nm in solution.[34] The transient absorption profiles indicated a fast rise, a fast decay, and a successive slow rise. The fast rise was assigned to the formation of CH_2I radical by direct dissociation. The fast decay with a time constant of 350 fs was assigned to disappearance of the CH_2I radical by primary geminate recombination in a solvent cage. The slow rise was assigned to a vibrational relaxation of the CH_2I radical. We observed similar time profiles at 400 nm upon excitation at 268 nm in acetonitrile (CH_3CN).[35] We assigned the fast rise and decay components to the instantaneous formation and decay of the CH_2I radical, but the slow rise com-

FULL PAPERS

ponent to a CT complex between the solute and the photo-fragment iodine. Tarnovsky et al. reported a similar transient absorption upon excitation of the B_1 state at 310 nm in acetonitrile.[36] They suggested the dynamics to be the electronically excited CH_2I_2 molecule, which stayed for 350 fs in a repulsive state, and slower photodissociation (0.35–1 ps) was proposed. The slow-rise component was considered to be due to the isomer CH_2–I–I. Kwok and Phillips studied the resonance Raman spectra upon excitation at the B_1 state and showed that the single C−I bond of CH_2I_2 was rapidly lengthened in 10–20 fs.[37a] The transient resonance Raman spectra showed overtone progressions, which were suggested to be the I–I stretching mode of isomer CH_2–I–I.[37b,c] The same authors observed a similar progression in the photoproduct of CH_3I in solution, but it was identified to the I–I stretching mode of CH_3–I–I complex formed by "solute CH_3I and fragment I".[37d] Several studies on the reaction dynamics of CH_2I_2 were recently conducted by time-resolved experiments,[38–41] that is, transient absorptions in solution[38] and supercritical fluids[40] and time-resolved X-ray diffraction in solution.[41] In these studies, interactions of fragments between CH_2I and I were investigated, and successive processes after the photodissociation were discussed for the formation of isomer CH_2–I–I.

The present study examines the photoinduced reactions of CH_2I_2 in acetonitrile and hexane by using subpicosecond and nanosecond transient absorption spectroscopy at room temperature. The transients produced upon excitation at 268 nm were probed from 340 to 740 nm. Time-resolved absorption spectra at around 340 nm were obtained from absorption immediately after photoexcitation (≤ 1 ps) and correspond to the reported CH_2I radical in the gas phase.[39,56] The slow-rise components were observed at all probed wavelengths, and the time constants were found to be significantly dependent on the concentration of CH_2I_2. The analysis of time-resolved absorption spectra and kinetics indicate that a CT complex, $CH_2I_2{}^{\delta+}\cdots I^{\delta-}$, is formed between the photofragment I atom and the solute CH_2I_2. We discuss this process on the basis of the concentration dependence of the slow-rise component and suggest that the reaction occurs in an environment of pre-existing solute aggregates.

Results and Discussion

Absorption Spectra of CH_2I_2 in solution

The static absorption spectra of CH_2I_2 in acetonitrile and hexane are shown in Figure 1. The spectra can be broken down into the sum of four Gaussian functions in the gas phase, as shown by the dashed lines. Each band has a similar bandwidth to that in the gas phase.[48a] This coincidence suggests that the initial process at the Franck–Condon excited region is nearly equivalent to that in the gas phase, which is often described by the direct (ultrafast) dissociation.[45–55] The peak positions underwent a blue shift by 1000 cm^{-1} in acetonitrile and a red shift by 700 cm^{-1} in hexane relative to that in the gas phase. Such shifts are commonly observed in

alkyl halides dissolved in solvents.[57,58] The excitation wavelength at 268 nm for CH_2I_2 corresponds mainly to the B_1 state in acetonitrile and to both the B_1 and A_1 states in hexane.

Dynamics of Transient Absorptions Observed in the Subpicosecond and Picosecond Regions

Figure 2 displays the transient absorptions in acetonitrile probed at several different wavelengths, from the UV to the near-IR region, within 5 ps. The insets show the absorptions within 50 ps. The transient absorptions observed in hexane are shown in Figure 3. All time profiles gave common characteristics: a fast rise, a fast decay, and a slow rise. As listed in Table 1, the best-fit time constants were obtained by fitting the time profiles with three exponential functions convoluted with the instrumental response function. The two fast time constants in acetonitrile are almost same as those in hexane within experimental error.[59]

Figure 4 shows the pump-power dependence of the transient absorptions at 500-fs and 20-ps delay times, probed at 400 nm in acetonitrile. The data indicate that the absorbances of the fast and slow rises are linearly proportional to the pump power. As a result, the transient dynamics seem to occur by a one-photon process. Taking into account excitation to the state of direct dissociation, we assigned the fast rise to generation of the CH_2I radical. The assignment is rationalized by the time-resolved absorption spectra in the
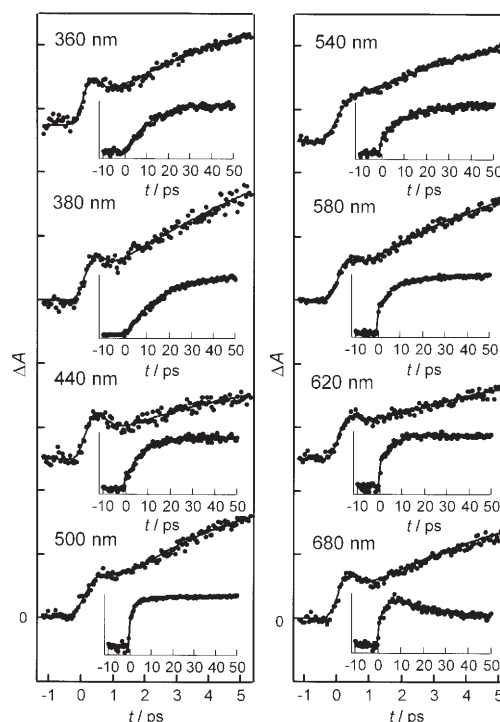

Figure 2. Transient absorption signals probed at eight different wavelengths for photoproducts of CH_2I_2 within 5 ps in acetonitrile. Insets: signals within 50 ps. The solid lines represent the best-fit results obtained by the three exponentials convoluted with the instrument response function.
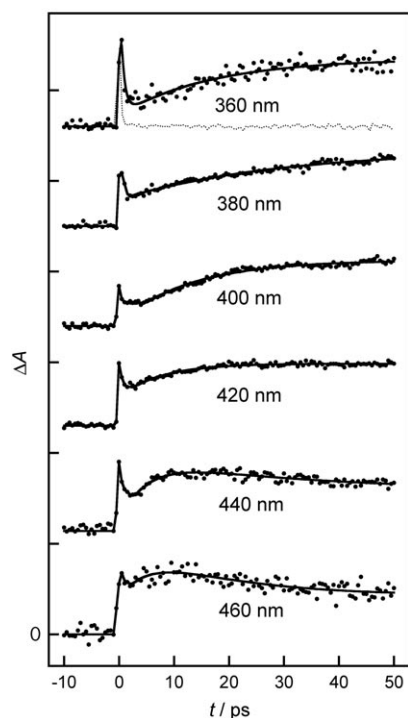
Figure 3. Transient absorption signals probed at six different wavelengths for photoproducts of CH$_2$I$_2$ within 50 ps in hexane. The solid lines represent the best-fit results obtained by the exponential function convoluted with the instrument response function. The dashed line is due to the solvent-induced artifacts.
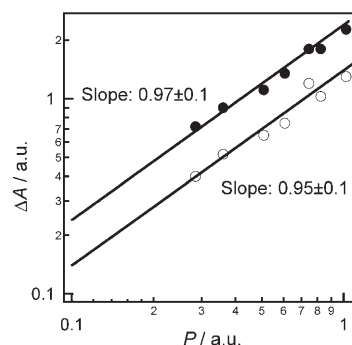

Figure 4. Pump-power dependence of the transient absorption signals probed at 400 nm in acetonitrile. ● = 20 ps, ○ = 500 fs.

subpicosecond region, because we recognized the absorption band of the CH$_2$I radical centered at 340 nm in the spectra, as described later. Thus, the CH$_2$I radical is generated immediately after photoexcitation, and the absorption rises instantaneously (Figure 2). Subsequently, the transient absorption decays, and the CH$_2$I radical disappears with a time constant of less than 500 fs. The most plausible mechanism for the disappearance of the CH$_2$I radical is primary geminate recombination.

Transient absorptions in the picosecond region were recorded as a function of solute concentration in both acetonitrile and hexane. The pump-probe signals within 5 ps in acetonitrile probed at 400 and 580 nm are shown in Figure 5,
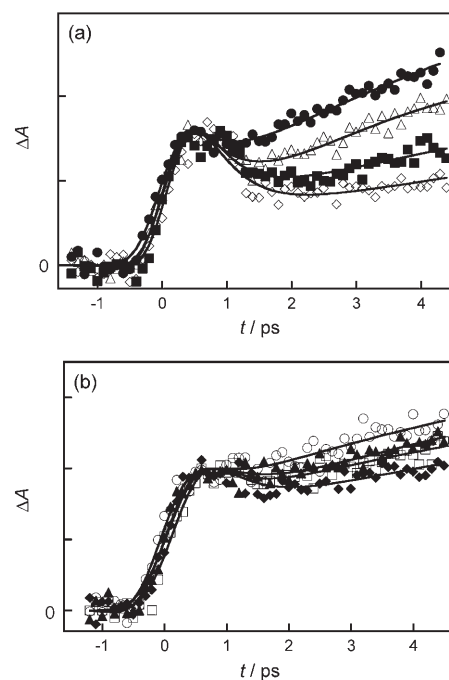
Table 1. Best-fit time constants of transient absorptions for photoproducts of CH$_2$I$_2$ in acetonitrile and hexane.

Solvent	λ [nm]	τ_1 (fast rise) [fs]	τ_2 (fast decay) [fs]	τ_3 (slow rise) [ps]
CH$_3$CN	360	190 ± 110	510 ± 120	10.1 ± 0.6
	380	210 ± 100	450 ± 110	13.9 ± 0.7
	400	200 ± 90	440 ± 120	7.3 ± 0.6
	420	200 ± 100	430 ± 140	6.8 ± 0.5
	440	210 ± 90	410 ± 150	6.2 ± 0.6
	460	180 ± 110	430 ± 140	3.5 ± 0.3
	480	190 ± 90	460 ± 160	3.1 ± 0.5
	500	220 ± 110	510 ± 170	3.1 ± 0.3
	520	210 ± 120	450 ± 130	6.7 ± 0.4
	540	220 ± 100	440 ± 130	9.2 ± 1.0
	560	200 ± 110	480 ± 150	7.2 ± 0.8
	580	210 ± 120	490 ± 160	6.5 ± 0.4
	620	200 ± 120	420 ± 120	5.1 ± 0.5
	640	200 ± 110	440 ± 110	4.9 ± 2.0
	680	190 ± 100	480 ± 120	4.6 ± 1.5
	740	210 ± 120	460 ± 140	4.3 ± 2.0
Hexane[a]	360	–[b]	–[b]	17 ± 1.7
	380	–	–	30 ± 3.0
	400	150 ± 80[c]	620 ± 200[c]	13 ± 1.2
	420	–	–	7.6 ± 0.6
	440	–	–	5.5 ± 1.5
	460	–	–	4.9 ± 2.0

[a] At longer wavelengths than 480 nm, transient absorptions were too weak to detect in hexane. [b] Fast components of transient absorption were not determined in hexane by artifacts arising from solvent. [c] Time constants for fast-rise and decay components at 400 nm in hexane were roughly obtained by subtracting artifacts of solvent from data of solution obtained under the same experimental conditions.

Figure 5. Transient absorption signals probed at a) 400 nm and b) 580 nm for photoproducts of CH$_2$I$_2$ within 5 ps at different concentrations in acetonitrile. In a), ● = 6.2 × 10^{-3}, △ = 2.5 × 10^{-3}, ■ = 1.2 × 10^{-3}, ◇ = 3.1 × 10^{-4} M. In b), ○ = 1.2 × 10^{-2}, ▲ = 6.2 × 10^{-3}, □ = 4.3 × 10^{-3}, ◆ = 2.5 × 10^{-3} M. The solid lines represent the best-fit results obtained by the exponential function.

and those within 50 ps at 400 nm in acetonitrile and hexane are shown in Figure 6. The fast rise and decay components at both red and blue bands are independent of the solute
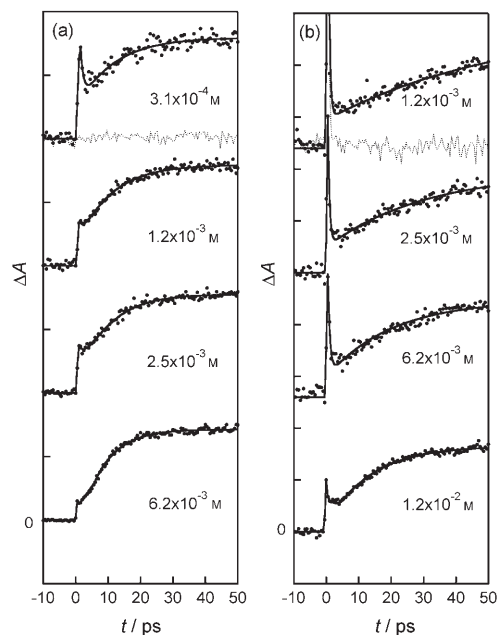

Figure 6. Transient absorption signals probed at 400 nm for photoproducts of CH_2I_2 within 50 ps in a) acetonitrile and b) hexane. The solute concentration is 3.1×10^{-4}–1.2×10^{-2} M. The solid lines represent the best-fit data obtained by the exponential function. The dashed lines are the signals from the neat solvents.

concentrations chosen in this experiment. On the other hand, the slow signal rises depend significantly on concentration in both solutions. These results seem to indicate that the slow rise does not arise from a photofragment, but reflects a solute-induced process. The time constants of these components are listed in Tables 2 and 3.

Transient Absorption Spectra on the Nanosecond Timescale

To assign the slow rise, we performed nanosecond transient absorption experiments with solutions in acetonitrile, hexane, and CH_2Cl_2. In Figure 7a, the solid line is the transient absorption spectrum of photoproducts in acetonitrile. The static absorption spectrum of the product by UV photolysis of CH_2I_2 in 3MP matrix at 77 K[27a] is shown by the dotted line. The spectrum in the nanosecond region is in good agreement with that in the 3MP matrix. Figure 7b shows the transient spectra recorded in hexane and CH_2Cl_2. These results indicate that similar transient absorption bands are formed in these solutions at room temperature and in the low-temperature matrices.[26, 27a, 28] Mohan et al. assigned the blue band to $CH_2I_2^+$ and explained that its formation was caused by electron transfer between two photo-excited CH_2I_2 molecules.[27a] This reaction scheme, however, cannot be accepted in the present study, because the slow-

Table 2. Best-fit time constants of transient absorptions for photoproducts of CH_2I_2 probed at 400 nm as a function of solute concentration.

Solvent	Conc. [M]	τ_1 (fast rise) [fs]	τ_2 (fast decay) [fs]	τ_3 (slow rise) [ps]
CH_3CN	3.1×10^{-4}	180 ± 110	480 ± 200	12.8 ± 1.8
	6.2×10^{-4}	190 ± 100	500 ± 190	11.5 ± 1.2
	1.2×10^{-3}	250 ± 150	540 ± 200	10.8 ± 0.8
	1.8×10^{-3}	170 ± 110	520 ± 260	9.8 ± 1.0
	2.5×10^{-3}	200 ± 100	400 ± 130	9.1 ± 0.6
	6.2×10^{-3}	160 ± 120	450 ± 200	7.4 ± 0.3
	9.3×10^{-3}	210 ± 100	530 ± 240	7.2 ± 0.6
	1.2×10^{-2}	170 ± 110	490 ± 240	7.1 ± 0.5
Hexane[a]	1.2×10^{-3}	–[b]	–[b]	51 ± 3
	1.8×10^{-3}	–	–	36 ± 2
	2.5×10^{-3}	–	–	30 ± 1
	6.2×10^{-3}	–	–	20 ± 1
	9.3×10^{-3}	–	–	15 ± 1
	1.2×10^{-2}	–	–	13 ± 1

[a] At concentrations lower than 1×10^{-3} M, transient absorption was too weak to detect in hexane. [b] Fast-rise and decay components in hexane could not be determined by artifacts of neat hexane.

Table 3. Best-fit time constants of transient absorptions for photoproducts of CH_2I_2 probed at 580 nm as a function of solute concentration in acetonitrile.

Conc. [M][a]	τ_1 (fast rise) [fs]	τ_2 (fast decay) [fs]	τ_3 (slow rise) [ps]
1.2×10^{-3}	–[a]	–[a]	9.7 ± 1.7
2.5×10^{-3}	180 ± 100	460 ± 170	8.5 ± 0.7
4.3×10^{-3}	220 ± 120	430 ± 160	8.1 ± 0.6
6.2×10^{-3}	190 ± 110	440 ± 140	7.7 ± 0.6
9.3×10^{-3}	210 ± 100	480 ± 130	7.4 ± 0.4
1.2×10^{-2}	200 ± 120	460 ± 160	6.7 ± 0.4

[a] At solute concentrations lower than 1.2×10^{-3} M, transient absorption was too weak to detect.

rise component showed a linear pump-power dependence (Figure 4).

As shown in Figure 8, the time profiles of the transient photoproducts probed at 400 and 580 nm consist of a rise within a pulse width of about 30 ns and an exponential decay with a time constant of about 100 ns. By using solutions before and after UV irradiation at 268 nm, a difference absorption spectrum was recorded (Figure 9a).[60] The spectrum in acetonitrile shows two bands in the UV and visible regions. Notably, the UV band is identical to the absorption spectrum of I_3^- as shown in the inset,[61] and the visible band at around 460 nm is identical to the spectrum of I_2 in acetonitrile. As a result, these bands are assigned to I_3^- and I_2, respectively.

To examine further the formation of the final photoproducts of I_3^- and I_2, the transient absorptions were recorded (Figure 9b and c). The transient probed at 480 nm decayed with time constants of about 50 and 650 ns. The transient absorption at 360 nm decayed with a time constant of about 50 ns and rose with one of about 600 ns. As the time constant of the rise component at 360 nm is similar to that of the second decay at 480 nm, the appearance of I_3^- seems to
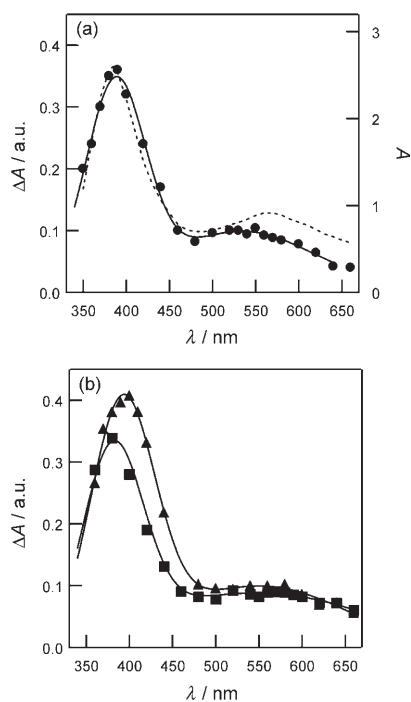
Figure 7. Nanosecond transient absorption spectra for the photoproduct of CH_2I_2 immediately after excitation with an XeCl excimer laser. a) The solid circles (●) and line (left vertical axis) are the transient absorption signals and fitting curve obtained by two Gaussian functions in acetonitrile at 293 K, respectively. The dashed line (right vertical axis) represents the static absorption spectrum of $CH_2I_2^+$ in 3MP matrix at 77 K reproduced from reference [27a]. b) The solid triangles (▲) and squares (■) are the transient spectra of the product in CH_2Cl_2 and hexane, respectively. The solid lines are the fitting curves obtained by two Gaussian functions.
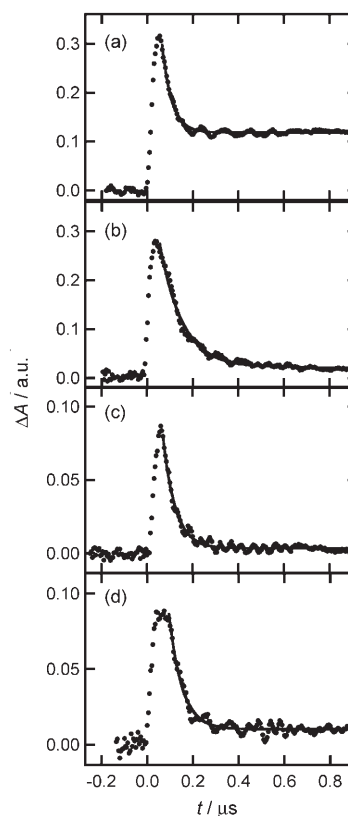

Figure 8. Time profiles of transient absorptions probed in the nanosecond region a) at 400 nm in acetonitrile, b) at 400 nm in hexane, c) at 580 nm in acetonitrile, and d) at 580 nm in hexane.

be correlated to the decay of I_2. We consider that I_3^- is generated by a reaction between I_2 and I^- through diffusion and equilibration processes in solution. It has been shown that the I_3^- ion is generated through $I_2 + I^- \rightleftharpoons I_3^-$ by dissolving I_2 and KI in polar solvents.[62] The ion I_3^- exists stably, and the stability of I_3^- was observed in the resonance Raman spectra of I_3^- and I_2.[63] The observation of I_3^- and I_2 was previously reported by warming the UV-irradiated matrix of CH_2I_2.[26b]

Transient Photoproducts Observed at Around 400 nm

By UV excitation, we observed two transient absorption bands centered at around 400 and 540 nm at room temperature. Similar absorption spectra at around 400 nm were reported by VUV excitation,[29] γ-ray[27b] irradiation of low-temperature matrices, and pulse radiolysis in solution.[30] From the experiment of the direct photoionization of CH_2I_2 upon excitation at 105 nm in Ar matrix at 15 K, the absorption spectrum of $CH_2I_2^+$ was observed at around 370 nm, which was identified by photoelectron spectroscopy to be the electronic transition A←X of $CH_2I_2^+$.[29] This assignment is in accordance with the result of nanosecond transient electroconductivity measurements.[30] In the present study, the absorption band at around 380 nm was obtained

by pico- and nanosecond transient absorption spectroscopy, and the photoproduct was generated by a one-photon process. The concentration-dependent slow rise indicates that the products that gave the band at around 400 nm are related to solute–solute interactions.

Simons and co-workers proposed that the absorption bands are associated with electrons trapped in clusters of polyhalomethane molecules in 3MP matrix.[26a,b] They suggested that the trapped electron is formed by electron transfer by tunneling between Rydberg orbitals of adjacent molecules.[26a] If trapped electrons were to be generated, the ejection of the electron should be much faster than the photodissociation. In the present study, the absorption at around 400 nm developed with time constants of 7–50 ps, depending on the solute concentration. This time range seems to be too long for electron ejection via the Rydberg state before the fast photodissociation process, which was calculated to be 8–80 fs in the gas[54,55] and solution states.[37a]

Another model was reported to be the isomer $CH_2–I–I$ formed by the reaction between CH_2I and I fragments after photodissociation.[28] As this isomerizaion is given by a single molecular process, the reaction should be independent of solute concentration. However, as shown in Figures 5 and 6, the slow-rise component depends significantly on solute concentration and becomes faster with increasing concentration. As for other reactions between CH_2I and I
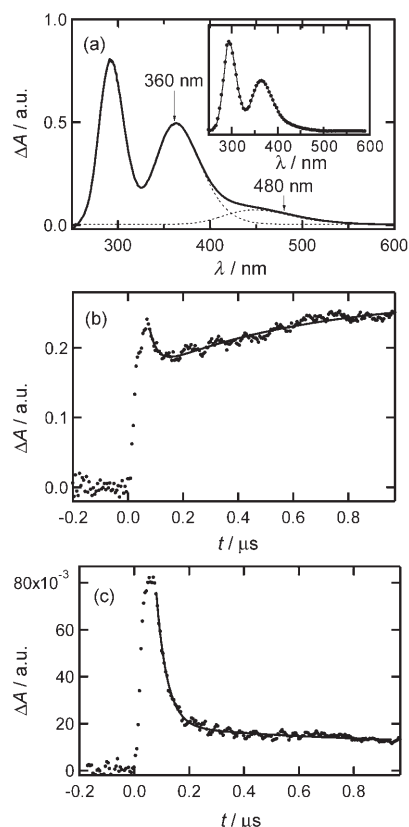
Figure 9. a) Difference absorption spectrum of CH_2I_2 in acetonitrile. The spectrum was obtained from the Lambert–Beer equation, that is, reference and sample solutions are those before and after UV irradiation, respectively. The experimental conditions are described in reference [60]. Inset: absorption spectrum of I_3^- reproduced from reference [63a]. b) Time profile of transient absorptions in acetonitrile probed in the nanosecond region at 360 nm. c) Time profile of above at 480 nm.

Figure 10. Time-resolved absorption spectra of the photoproduct of CH_2I_2 in acetonitrile at four different delay times. The solid lines are the best fits obtained by three Gaussian functions. The dashed spectra are assigned to the CH_2I radical (340 nm), the ion pair $CH_2I_2^+\cdots I^-$ (385 nm), and the CT complex $CH_2I_2^{\delta+}\cdots I^{\delta-}$ (430 nm).

Figure 11. Time profiles of the transient absorptions in acetonitrile probed at 400 nm. Two profiles are reproduced from the transient absorption bands deconvoluted with two Gaussian functions assigned to the CT complex (○) and the ion pair (●).

fragments, the following studies were reported. The recombination to the parent CH_2I_2 molecule, in contrast to the formation of $CH_2–I–I$, gains much energy, on the order of about 15 000 cm^{-1}.[32] The potential well for the formation of the parent molecule is seven times deeper than the almost-flat well for the formation of the isomer.[33] These two studies represent fragments that preferably combine to re-form the parent molecule.

Origin of Slow-Rise Component after Photodissociation

We constructed time-resolved absorption spectra at around 400 nm with the results shown in Figure 10. The spectra are well-fitted by three Gaussian functions, which have peaks at 340, 385, and 430 nm. The absorption at around 340 nm grew first. It was observed that the CH_2I radical has a broad absorption band in the UV-to-blue region and is centered at around 340 nm in the gas phase.[39,56] Thus, the first generated band was assigned to the CH_2I radical immediately after photodissociation through direct dissociation. Second, the transient at around 430 nm gradually grew, and Figure 11 shows that the band at 430 nm grew faster than that at
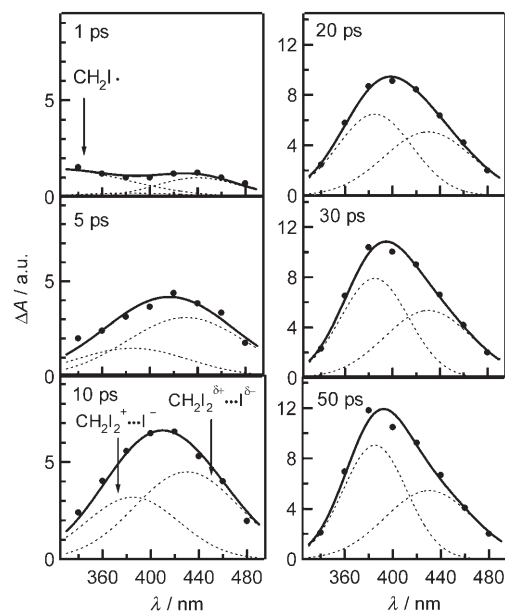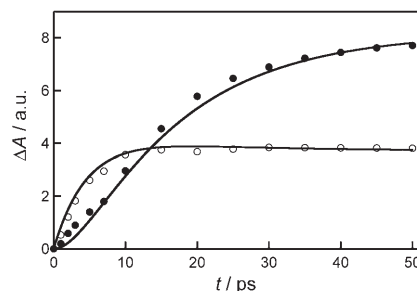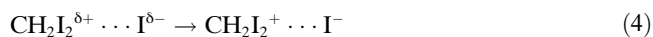
385 nm. It seems that the band at 430 nm is the precursor of the photoproduct at 385 nm. We then examined a model in which the slow-rise component represents a reaction to form a CT complex, $CH_2I_2^{\delta+}\cdots I^{\delta-}$, between the photofragment I and the solute CH_2I_2. The CT complex then proceeds further to an ion-pair state.

CT absorption bands with a halogen atom as an electron acceptor have been known to show a sublinear correlation between the absorption peak and the ionization potential of the donor molecule.[9–12] The energy correlation of CT complexes that consist of an iodine atom and alkyl iodides has been reported.[65,66] By using these correlations, the CT complex is expected to have an absorption at around 430 nm. This coincides exactly with the band at around 430 nm in

Figure 10. Thus, we propose the following reaction mechanism for the photoexcitation of CH_2I_2 (Equations (1)–(4)):

$$CH_2I_2 \xrightarrow{h\nu} CH_2I + I \tag{1}$$

$$CH_2I + I \rightarrow CH_2I_2 \tag{2}$$

$$CH_2I_2 + I \rightarrow CH_2I_2{}^{\delta+} \cdots I^{\delta-} \tag{3}$$

$$CH_2I_2{}^{\delta+} \cdots I^{\delta-} \rightarrow CH_2I_2{}^{+} \cdots I^{-} \tag{4}$$

Equation (1) represents the generation of a CH_2I radical by direct photodissociation, and it is followed by primary geminate recombination as shown in Equation (2). These steps are observed as the fast rise and decay of the transient absorptions. Some of the I fragments escape from geminate recombination and form a CT complex with CH_2I_2 in Equation (3). Equation (4) expresses the generation of an ion pair as the final product on the picosecond timescale. The slow rises show a subsequent formation of and a full electron transfer from the CT complex. The free-energy gap (ΔG) before and after the electron-transfer process is less than -0.2 or -1 eV, depending on whether the fragment is I or I*.[67] The reaction between iodine and solute CH_2I_2 is the most plausible rationalization for the experimental results: pump-power dependence, concentration dependence, time profiles of the transient absorptions, and time-resolved absorption spectra.

Several reports provided similar examples to the above reaction schemes. Barbara and co-workers found the generation of a benzene cation in solution by electron transfer via the CT state from benzene to the photolyzed Br by using ultrafast spectroscopy.[14] Bühler and co-workers found that the rise component of the transient absorption of a CT complex of a polyhalomethane becomes faster as the solute concentration increases.[70] CT complexes and ion pairs, with a strong dipolar intermediate as charge-transferred or charge-separated products, give intense absorptions; that is, the extinction coefficient of the photoproduct of CH_2I_2 ($\varepsilon_{max} = 10\,000\,M^{-1}\,cm^{-1}$ at 380 nm[28b]) is greater than those of neutral molecules ($\varepsilon_{max}(CH_2I_2) = 1200\,M^{-1}\,cm^{-1}$ at 300 nm,[48a] $\varepsilon_{max}(CH_2I$ radical$) = 850\,M^{-1}\,cm^{-1}$ at 340 nm[56]). Under such conditions, the weak absorption of the CH_2I radical is masked considerably by the intense absorption given by successive reactions after photodissociation.

We consider that the ion pair is formed through electron transfer of the CT complex in the picosecond region by UV photolysis of CH_2I_2 in solution. The separated ion I^- allows the generation of I_3^- together with I_2,[62,63] as shown by the rise of the I_3^- band and the decay of the I_2 band in the nanosecond region. A similar observation was reported during the warming of the UV-irradiated matrix of CH_2I_2.[26b] In that study, the absorption at around 400 nm disappeared, whereas the absorption bands of I_3^- and I_2 alternately appeared by a diffusion process during softening. This result is consistent with the assumption that the band at around 400 nm is due to a precursor of I_3^-. In solution, I_3^- was re-

cently observed by nanosecond transient absorption upon excitation of CH_2I_2 at 266 nm in CH_3CN and alcohols.[38] In this study, the principal precursor of I_3^- is described as I^-, which is given by the reaction $CH_2I–I \rightarrow CH_2I^+ + I^-$.

We now briefly discuss the other results of femtosecond transient absorption spectroscopy. Harris and co-workers assigned the slow-rise component to vibrational relaxation of CH_2I radical.[34] The reason for this assignment was as follows. First, the time constant matches the typical vibrational relaxation time of a small molecule in solution.[4] Second, the probe wavelength was reported to be nearly the peak position of the absorption band of the radical.[27b] Generally, the transient absorption probed at its absorption maximum rises and decays at its band edges by vibrational cooling. If a slow-rise component was responsible for the vibrational cooling process, the decay component should have been observed at the absorption edge. As shown in Figure 3, however, the third component rose at the blue and red edges within 5 ps, and these slow rises were observed in the whole range of observation from UV to near-IR.

Tarnovsky et al. ascribed the two fast components and the slow component to the electronically excited CH_2I_2 molecule, which stayed for 350 fs in a repulsive state, and a slow photodissociation was proposed.[36] First, the proposed dissociation time (0.35–1 ps) seems to be too long for the direct dissociation studied by numerous authors (see above).[34,35,37a,45–55] Second, we consider the relationship of the dissociation rate and the absorption band. The analytically decomposed bands (the first and second B_1 and A_1 bands) recorded in the present solutions are almost the same as those in the gas phase,[48a] in which direct dissociation takes place; that is, the differences in solution and gas phase of these bands are within 4 %. Third, the experimental results shown in Figures 5 and 6 indicate that the slow rise becomes faster as the solute concentration increases. These concentration-dependent time profiles cannot be applied to the isomer, because the isomer reaction is caused by a single molecular process.

Formation of Charge-Transfer Complex in Solute Aggregates

We observed the formation of the CT complex after photodissociation in the picosecond region. If the solution is homogeneous, this timescale seems to be too short for the encounter of the fragment I and the solute CH_2I_2 in the present concentration range (10^{-4}–10^{-2} M). According to Equation (5), we confirm the encounter time τ of two species:[71]

$$\tau = l^2 D^{-1} \tag{5}$$

in which l is the average distance between CH_2I_2 and I, and D is the sum of the two diffusion constants.[35] The estimated time lies between 5 and 100 ns in the present experimental concentration range, which is sharply different from the observed values, which lies in the 7–50 ps range. Accordingly, this suggests that the solute CH_2I_2 is not homogeneously dis-

solved in solution. The inhomogeneity of the solute molecules is generally driven by strong solute–solute interactions.

We now describe the intrinsic and specific properties of CH_2I_2. It is known that the van der Waals energy is formulated by Equation (6):[72]
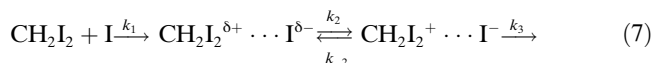
$$W = \frac{A}{12\pi D_0} = 2\gamma \tag{6}$$

in which W is the van der Waals energy, A is the Hamaker constant, D_0 is the contact intermolecular distance, and γ is the surface energy. Notably, the γ value of CH_2I_2 is the largest among 450 organic liquids:[73,74] $\gamma(CH_2I_2) = 67$, $\gamma(H_2O) = 73 \text{ mJ m}^{-2}$ at 298 K. Furthermore, the vaporization energy was also reported to be large: $\Delta H_{vap}(CH_2I_2) = 45.6 \text{ kJ mol}^{-1}$[75] at 298 K, which is similar to that for water, $\Delta H_{vap}(H_2O) = 45.0 \text{ kJ mol}^{-1}$. In other words, the CH_2I_2 molecule has strong intermolecular interactions. These strong interactions seem to play an important role in forming the structure of CH_2I_2 in solution. In fact, the structure around CH_2I_2 solute was investigated by Raman spectroscopy, and a very large spectral shift (20 cm^{-1}) of the C–H stretching of CH_2I_2 was observed when the concentration of CH_2I_2 was increased.[64] In that study, the aggregation tendency of CH_2I_2 solute was clear at room temperature, because the evaluated microscopic concentration became higher than the macroscopic one. Another specific feature of CH_2I_2 was reported in terms of the solubility of polyhalomethanes. According to the Hildebrand parameter, the CH_2I_2 molecule is said to be the most insoluble solute in various polyhalomethanes.[26a] We observed "phase separation" in concentrated solutions of CH_2I_2, for example, when the concentration of CH_2I_2 was greater than 0.1 M in hexane.

On the basis of the following five reasons, we introduce the aggregation of CH_2I_2 to explain the fast formation of the CT complex. First, the fragment I readily finds a partner CH_2I_2 in aggregates within a few tens of picoseconds. Second, the aggregation of CH_2I_2 in solution at room temperature is indicated by Raman spectroscopy.[64] Third, it has been suggested that the formation of $CH_2I_2^+$ in matrix is due to solute interactions with a sublinear dependence of absorbance on concentration.[27a] Fourth, the CH_2I_2 molecule is the most insoluble solute in various polyhalomethanes.[26a] Fifth, the very large van der Waals energy of CH_2I_2 is in favor of aggregate formation.

Kinetics of Sequential Reactions After Photodissociation

Figure 11 shows two time profiles in acetonitrile at 400 nm. These were reproduced from the time-resolved absorption bands analyzed by two Gaussian functions (Figure 10) and were assigned to the CT complex and the ion-pair complex. It is clear that the former is formed faster than the latter. We analyzed the kinetics for CT-complex formation and the electron-transfer process as follows (Equation (7)):

$$CH_2I_2 + I \xrightarrow{k_1} CH_2I_2{}^{\delta+}\cdots I^{\delta-} \underset{k_{-2}}{\overset{k_2}{\rightleftharpoons}} CH_2I_2{}^+\cdots I^- \xrightarrow{k_3} \tag{7}$$

in which k_1, k_2, k_{-2}, and k_3 represent each reaction rate constant. In this scheme, photodissociation and geminate recombination are not included, because these processes are completed within a few hundred femtoseconds, and the influence on CT-complex formation and later processes is minute. We introduced the back reaction of the electron transfer, because the transient absorption of the CT complex showed a small decay component in the time range of observation regardless of the rise of the $CH_2I_2^+\cdots I^-$ band. This behavior indicates that formation of the ion pair from the CT complex may cause a back reaction in the above scheme.

We analyzed the reaction in Equation (7) by solving the following rate equations (Equations (8)–(10)):

$$\frac{d[I]}{dt} = -k_1[CH_2I_2][I] \tag{8}$$

$$\frac{d[CH_2I_2{}^{\delta+}\cdots I^{\delta-}]}{dt} = \\ k_1[CH_2I_2][I] - k_2[CH_2I_2{}^{\delta+}\cdots I^{\delta-}] + k_{-2}[CH_2I_2{}^+\cdots I^-] \tag{9}$$

$$\frac{d[CH_2I_2{}^+\cdots I^-]}{dt} = \\ k_2[CH_2I_2{}^{\delta+}\cdots I^{\delta-}] - k_{-2}[CH_2I_2{}^+\cdots I^-] - k_3[CH_2I_2{}^+\cdots I^-] \tag{10}$$

Under the present experimental conditions, such as photon flux and solute concentration, the pump pulse of 268 nm excited CH_2I_2 by less than 1% in the irradiated volume. This means that the number of ground-state molecules is much greater than the number of fragments I. Accordingly, the CT-complex formation can be safely approximated to a pseudo-first-order reaction. Here, we introduce a local concentration $[CH_2I_2]_L$, which reflects the number of CH_2I_2 molecules around the photofragment I, instead of the macroscopic bulk concentration $[CH_2I_2]$ (see next section). In Equation (10), the first two terms proceed in the picosecond time region. On the other hand, the third term takes several tens of nanoseconds. As the former two terms are so large that the third term can be neglected, the above rate equations can be safely reduced to the following (Equations (11)–(13)):

$$\frac{d[I]}{dt} = -k_1'[I] \tag{11}$$

$$\frac{d[CH_2I_2{}^{\delta+}\cdots I^{\delta-}]}{dt} = k_1'[I] - k_2[CH_2I_2{}^{\delta+}\cdots I^{\delta-}] + k_{-2}[CH_2I_2{}^+\cdots I^-] \tag{12}$$

$$\frac{d[CH_2I_2{}^+\cdots I^-]}{dt} = k_2[CH_2I_2{}^{\delta+}\cdots I^{\delta-}] - k_{-2}[CH_2I_2{}^+\cdots I^-] \tag{13}$$

in which k_1' is defined as $k_1[CH_2I_2]_L$.

To solve the above rate equations, we use the matrix method.[76] The results are as follows (Equations (14)–(16)):

$$[I]_t = [I]_0 \exp(-k_1't) \tag{14}$$

$$[CH_2I_2^{\delta+} \cdots I^{\delta-}]_t =$$
$$[I]_0 \left[\frac{k_{-2}}{k_2 + k_{-2}} + \frac{k_{-2} - k_1'}{k_1' - k_2 - k_{-2}} \exp(-k_1't) \right. \tag{15}$$
$$\left. + \frac{k_1'k_2 \exp\{-(k_2 + k_{-2})t\}}{(k_2 + k_{-2})(k_1' - k_2 - k_{-2})} \right]$$

$$[CH_2I_2^{+} \cdots I^{-}]_t =$$
$$[I]_0 \left[\frac{k_2}{k_2 + k_{-2}} + \frac{k_2}{k_1' - k_2 - k_{-2}} \exp(-k_1't) \right. \tag{16}$$
$$\left. - \frac{k_1'k_2 \exp\{-(k_2 + k_{-2})t\}}{(k_2 + k_{-2})(k_1' - k_2 - k_{-2})} \right]$$

Using Equations (15) and (16), we fitted the time profiles of the transient absorptions for the slow-rise component at a concentration of 10^{-2} M. As shown in Figure 11, the experimental results are in good agreement with the above kinetics, that is, the kinetics of the CT complex and ion pair are consistent with the above reaction scheme. We obtained the rate constants $k_1' = (2.4 \pm 0.3) \times 10^{11}$, $k_2 = 7.0 \times 10^9$, and $k_{-2} = 5.8 \times 10^{10}$ s^{-1}. As the rate constant k_1' is much greater than k_2 and k_{-2}, the CT-complex formation is the major process in the reaction in Equation (7).

Difference in Macroscopic Bulk Concentration and Microscopic Local Concentration in Two Typical Solutions

In both acetonitrile and hexane, the slow-rise component of the transient absorption becomes faster nonlinearly as the CH_2I_2 concentration increases. In other words, although the time constant in hexane is about five times greater than that in acetonitrile at 10^{-4} M, the difference decreases at higher concentrations. Here, we mention that the aggregate corresponds to an ensemble of solute molecules of an undefined number, unlike a specific dimer. If only a dimer was responsible for the CT-complex formation, the formation rate could have been exclusively determined independent of the solute concentration. The degree of aggregation or locally enhanced concentration makes the formation of the CT complex faster. We consider that these features represent how solutes are aggregated at a given concentration in acetonitrile and hexane.

To investigate aggregation, the local concentration $[CH_2I_2]_L$ is estimated in the following manner. The transient absorption bands of the CT complex and ion pair overlap as shown in Figure 11. First, the signal intensity at 400 nm, $I(t,400)$, is described as in Equation (17):

$$I(t,400) = I_{CT}(t, 400) + I_{IP}(t, 400)$$
$$= \varepsilon_{CT}(400)[CH_2I_2^{\delta+} \cdots I^{\delta-}]_t + \varepsilon_{IP}(400)[CH_2I_2^{+} \cdots I^{-}] \tag{17}$$

in which $\varepsilon_{CT}(400)$ and $\varepsilon_{IP}(400)$ are the extinction coefficients of the CT complex and ion pair, respectively. By using $[CH_2I_2^{\delta+} \cdots I^{\delta-}]_t$ and $[CH_2I_2^{+} \cdots I^{-}]_t$ given by Equations (15) and (16) and the signal intensities in Figure 11, the ratio of the extinction coefficient at 400 nm, $\varepsilon_{IP}(400)/\varepsilon_{CT}(400)$, was estimated to be a constant value of around 14 in the present time region. Second, we assume the three rate constants, k_1, k_2, and k_{-2}, determined in the above section, to be constant independent of bulk concentration and solvent. Third, the time profiles of the transient absorptions at the several bulk concentrations are fitted by Equation (17). As a result, the fitting parameter in Equation (17) is the only local concentration $[CH_2I_2]_L$, because all the rate constants except for k_1' are defined to be concentration independent. As we cannot obtain the absolute value of k_1, the local concentrations thus evaluated become relative values.

Figure 12 shows the local concentration $[CH_2I_2]_L$ as a function of the bulk concentration in both solutions. The local concentration in acetonitrile increased steeply with an
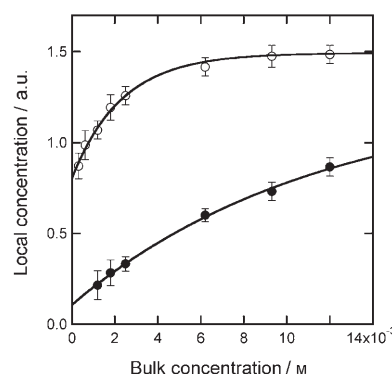

Figure 12. Evaluated local concentration of CH_2I_2 as a function of bulk concentration in acetonitrile (○) and hexane (●).

increase in macroscopic bulk concentration and became saturated at a relatively low bulk concentration. On the other hand, in hexane the local concentration increased monotonically and did not reach a plateau within the present range of experimental concentrations. As the local concentration increases, the effective number of CH_2I_2 molecules with which the photofragment I can generate a CT complex increases. Such a condition is established at a lower concentration in acetonitrile than in hexane. This means that the aggregate does not grow to more than a given size in acetonitrile, whereas it continues to develop in hexane. In fact, in concentrated solutions of hexane, phase separation takes place, but it does not occur at the higher concentrations in acetonitrile. The aggregation of CH_2I_2 solute can be stabilized by the polarization effect of solvent molecules.

In conclusion, we determined that the CT complex $CH_2I_2^{\delta+} \cdots I^{\delta-}$, generated in pre-existing aggregates of CH_2I_2, plays an important role in reactions of CH_2I_2 in solution and low-temperature matrices. The CT complex corresponds to a precursor of I_3^-, whose product is given by I^- and I_2

(Figure 9). These successive reactions after the photodissociation of CH_2I_2 are triggered by reactions with locally enhanced solute concentrations. In 1969, Simons and co-workers observed the generation of I_3^- by photolysis of CH_2I_2 in low-temperature matrices and reported the reactions in solute aggregates.[26a,b] In the present study, the experimental results show that solute aggregation plays an important role in the reactions of CH_2I_2 in room-temperature solutions too. Consequently, it was concluded that the CT complex $CH_2I_2^{\delta+}\cdots I^{\delta-}$, generated in pre-existing aggregates of CH_2I_2, is an intermediate of successive reactions after the photodissociation of CH_2I_2. This is the reason that the CT complex has not yet been considered as a candidate for an intermediate immediately after the photodissociation of CH_2I_2, except in our publications.

Assignment of Photoproduct of Transient Absorption Band at Around 540 nm

We measured the concentration dependence of transient absorptions at the red band in acetonitrile. Figure 6b shows the dynamics probed at 580 nm within 5 ps at several concentrations. The concentration range of CH_2I_2 is 2.5×10^{-3}–1.2×10^{-2} M. The general time profiles and concentration dependence are very similar to those observed for the blue band. The transient signals were also fitted by three exponential functions convoluted with the instrument response function. The obtained time constants of the fast rise, fast decay, and slow rise are listed in Table 2. As the dynamics of the fast components are independent of solute concentration, the fast rise and decay were assigned to the generation and disappearance of the photofragment CH_2I, respectively. This assignment is consistent with the ultrafast formation of the CH_2I radical observed at 620 nm by Harris and co-workers.[34] The slow components became faster as the concentration increased. This indicates a successive reaction between fragment and solute molecules.

As for the time profile in the longer time region, the transient absorptions were measured within 500 ps at 380 nm (blue band) and 540 nm (red band) in acetonitrile (Figure 13). The dynamics observed at 380 nm gave two rise components of (14 ± 1) and (160 ± 10) ps. On the other hand, the dynamics at 540 nm decayed with a time constant of (170 ± 20) ps. Thus, the time profile at the blue band is evidently different from that at the red band on the subnanosecond timescale. Furthermore, the time constant of the second rise component at 380 nm is nearly equal to that of the decay at 540 nm. On the basis of these experimental results, we discuss several candidates for a product at 540 nm and propose a new possible mechanism for the formation of the dimer cation.

We briefly discuss the alternative mechanisms in the literature. Formation of an isomer CH_2–I–I was proposed.[28] As this isomer is generated by a single molecular process, the formation dynamics should be independent of solute concentration. Therefore, this reaction cannot explain the present experimental results of concentration dependence. Fur-
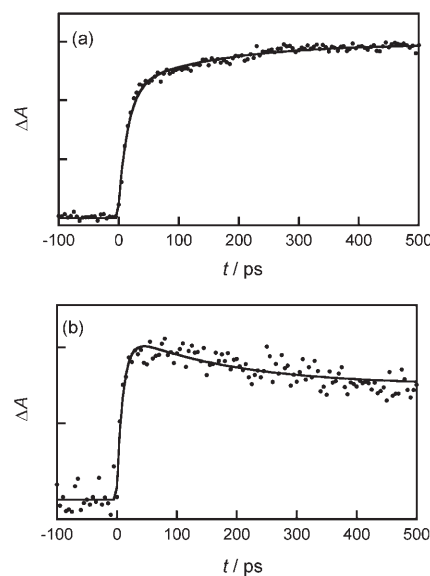

Figure 13. Time profiles of the transient absorptions on the subnanosecond timescale probed at a) 380 nm and b) 540 nm centered at the peak positions of both bands in acetonitrile. The time constant of the second rise component at 380 nm is nearly equal to that of the decay at 540 nm.

thermore, it cannot describe the coincidence of the time constant of the second rise observed at 380 nm with that of the decay observed at 540 nm on the subnanosecond timescale. As for other species, formation of a trapped electron was proposed.[26a,b] In the present study, the development of the absorption of the red band took about 10 ps. This timescale seems to be too long for the ejection of electrons before the much faster photodissociation process.

On the basis of the experimental results in the present study, the formation of the dimer cation was tentatively proposed to be via a CT complex between solute dimer and fragment I, followed by electron transfer. The increase in solute concentration raises the concentration of the dimer. As the dimer concentration increases, the photofragment I rapidly finds the dimer to generate the CT complex. These concentration dependences were suggested to be observed as a concentration-dependent slow rise (Figure 6b). If a part of the dimer cation is relaxed to a cation and a neutral species in the subnanosecond time region, the transient absorption of the blue band rises and that of the red one decays (Figure 13). Thus, we consider that a dimer cation is a possible candidate for producing the band at around 540 nm. The absorption spectra of dimer cations of various alkyl iodides were recorded as a function of solute concentration in solution.[42] It was clearly shown that the peak of absorption for the dimer cation is located at a longer wavelength than that for the cation, that is, the cation peak appears in the UV region, and dimer cation peak appears in the visible region.

Conclusions

The photoinduced reaction dynamics of CH$_2$I$_2$ in acetonitrile and hexane have been studied by time-resolved absorption spectroscopy from the subpicosecond to the nanosecond timescale over a wide wavelength region. The transient absorptions consist of three time components. A fast rise ($\tau \leq 200$ fs) and fast decay (≈ 500 fs) at around 400 nm were assigned to the generation of a CH$_2$I radical by direct photodissociation of CH$_2$I$_2$ and disappearance by primary geminate recombination, respectively. A concentration-dependent slow rise with time constants of 7–50 ps was observed at 400 nm. It was assigned to the formation of a CT complex (CH$_2$I$_2$$^{\delta+}\cdots$I$^{\delta-}$) between CH$_2I_2$ and photofragment I based on the concentration-dependent time-resolved absorption spectra in the picosecond region. This process was followed by a full electron transfer from CH$_2$I$_2$ to I to generate an ion-pair complex. The kinetics were analyzed by sequential formation of a CT complex and an ion-pair complex. In this scheme, a significant role for solute aggregation was proposed. We analyzed the results of the concentration-dependent slow rise by using rate constants to investigate the local structure around the CT complex, and the difference between macroscopic and microscopic concentrations was represented in both solutions. The analysis proposed that only CH$_2$I$_2$ in the neighboring region of initially photoexcited CH$_2$I$_2$ participates in CT-complex formation. Such a condition is more readily achieved at lower concentrations in acetonitrile than in hexane.

We also observed that the photoproduct gave an absorption band at around 540 nm. This band had a similar time profile to the blue band in the sense that the slow-rise component became faster with increasing concentration. We tentatively assigned this transient to a charge-separated species of the dimer cation and I$^-$. It was considered that CH$_2$I$_2$ solute interactions strongly influence the chemical processes after photoexcitation. Our results show that, even in solution at room temperature, the pre-existing solute aggregates govern the early dynamics.

Experimental Section

Subpicosecond Transient Absorption Spectrometer and Its Experimental Procedures

The optical configurations for the UV subpicosecond transient absorption spectrometer are described elsewhere.[35,77,78] Briefly, the light source was based on a regenerative amplified Ti/sapphire laser. A Ti/sapphire oscillator (Clark-MXR NJA-4) pumped by a position-stabilized Ar ion laser (Spectra Physics BeamLok 2060) produced an optical pulse width of 70 fs with an average power of 400 mW at 800 nm. The output pulse of the oscillator was temporally chirped by a stretcher and its energy per pulse was regeneratively amplified by a CW Q-switched intracavity-doubled Nd/YAG laser (Clark MXR ORC-1000) with 8-W output. With a pulse compressor, we finally obtained an amplified pulse with a pulse energy of 900 μJ at 800 nm with a pulse width of 120 fs at a repetition rate of 1 kHz (Clark MXR CPA-1000).

The fundamental output pulse was used to generate both a third harmonic (268 nm) as a pump pulse and a white-light continuum as a probe pulse. The fundamental pulse was passed through a BBO (β-barium borate) crystal (type I, thickness 1 mm) to generate a second harmonic (400 nm). After the second harmonic pulse was separated with a dichroic mirror, the polarization was rotated by a half-wave plate. The second harmonic and fundamental pulses were mixed on another BBO crystal (type I, thickness 0.5 mm) to generate a third harmonic pulse. This was passed through a pair of prisms to compensate for its group velocity dispersion and was separated from the fundamental and second harmonic pulses. The white-light continuum was generated by focusing the fundamental or the second harmonic pulse onto a quartz flow cell containing D$_2$O with a path length of 10 mm. The available wavelength regions for the probe light with the second harmonic and fundamental pulses were 340–600 and 500–900 nm, respectively. The configuration of linear polarization between the pump and the probe pulses was set to be the magic angle.

The pump pulse was loosely focused onto a quartz sample flow cell with a path length of 1 mm, and the energy in front of the cell was about 10 μJ. For the probe and reference pulses, the most stable part of the white-light continuum, selected by focusing it onto a pin hole, was used as the spatially stable part. The probed wavelength was selected with a suitable interference filter (Andover, full width at half maximum = 10 nm). The probe and reference pulses were detected by Si pin photodiodes. These signals were processed by two boxcar integrators (Stanford Research Systems SR250) and sent to an analogue processor (Stanford Research Systems SR235) to normalize the fluctuations of the white-light continuum on every laser shot. Finally, the normalized signals were processed by a third boxcar integrator operating in toggle mode. We were able to obtain directly absorbance changes by chopping pump pulses on every other shot. The absorbance change at a certain time delay on a computer-controlled stage was accumulated in a computer. The present transient absorption spectrometer allowed us to detect an absorbance change of $\Delta OD = 1 \times 10^{-4}$. The instrument response assumed with a Gaussian function was estimated to be 550 fs from the instantaneous rise of the excited-state absorption or instantaneous bleach for rhodamine 6G in ethanol and *p*-terphenyl in cyclohexane, depending on the probe wavelength.

Nanosecond Flash Photolysis

Transient absorption signals on the nanosecond timescale were measured by a system described elsewhere.[79] Briefly, pump and probe pulses were obtained from an XeCl excimer laser (308 nm; Lambda Physik EMG 101 MSC) and a xenon flash lamp (EG&G FX279U), respectively. The two pulses were triggered by a pulse generator (Hewlett Packard 8015A) at 1 Hz. Synchronization between the pump and probe pulses was carried out by a delay generator (Stanford Research Systems DG535). The probe beam that passed through a sample cell was directed onto a monochromator (Ritsu MC 10N) equipped with a photodiode. Signals were amplified with a fast amplifier (Stanford Research System SR445), processed with a programmable digitizer (Tektronix 7612D), and accumulated in a computer.

Samples

CH$_2$I$_2$ (Tokyo Kasei, >99%), hexane, acetonitrile, and dichloromethane (CH$_2$Cl$_2$; Wako, HPLC grade) were used as obtained. Sample solutions were flowed through a tube attached to a bottle of solution to ensure a fresh sample on every laser shot. Air was removed from the solutions by bubbling argon gas, and the solutions were replaced at intervals of a few hours to avoid degradation by laser irradiation.

Acknowledgements

K.-i. Saitow, K. Yoshihara et al.

[1] a) D. Raftery, R. J. Sension, R. M. Hochstrasser in *Activated Barrier Crossing* (Eds.: G. R. Fleming, P. Hänggi), World Scientific, London, **1993**; b) J. Schroeder, J. Troe in *Activated Barrier Crossing* (Eds.: G. R. Fleming, P. Hänggi), World Scientific, London, **1993**.

[2] G. R. Fleming, *Chemical Applications of Ultrafast Spectroscopy*, Oxford University Press, New York, **1986**.

[3] B. J. Schwartz, J. C. King, C. B. Harris in *Ultrafast Dynamics of Chemical Systems* (Ed.: J. D. Simon), Kluwer Academic Publishers, Dordrecht, **1994**.

[4] W. Kaiser, *Ultrashort Laser Pulses*, Springer-Verlag, New York, **1992**.

[5] A. L. Harris, J. K. Brown, C. B. Harris, *Annu. Rev. Phys. Chem.* **1988**, *39*, 341–366, and references therein.

[6] J. T. Hynes, *Annu. Rev. Phys. Chem.* **1985**, *36*, 573–597.

[7] D. E. Smith C. B. Harris, *J. Chem. Phys.* **1987**, *87*, 2709–2715.

[8] X. Xu, S.-C. Yu, R. Lingle, Jr., H. Zhu, J. B. Hopkins, *J. Chem. Phys.* **1991**, *95*, 2445–2457.

[9] M. Tamres, R. L. Strong in *Molecular Association*, *Vol. 2* (Ed.: R. Foster), Academic, London, **1979**, p.331, and references therein.

[10] R. S. Mulliken, W. B. Person, *Molecular Complexes*, Wiley-Interscience, New York, **1969**.

[11] J. Yarwood, *Spectroscopy and Structure of Molecular Complexes*, Prenum Press, London, **1973**.

[12] a) R. E. Bühler, *J. Phys. Chem.* **1972**, *76*, 3220–3228; b) R. E. Bühler M. Ebert, *Nature* **1967**, *214*, 1220–1221; c) R. E. Bühler, *Radiat. Res. Rev.* **1972**, *4*, 233–258, and references therein.

[13] a) D. Raftery, M. Iannone, C. M. Phillips, R. M. Hochstrasser, *Chem. Phys. Lett.* **1993**, *201*, 513–520; b) D. Raftery, E. Gooding, A. Romanovsky, R. M. Hochstrasser, *J. Chem. Phys.* **1994**, *101*, 8572–8579.

[14] a) W. Jarzeba, K. Thakur, A. Hoermann, P. F. Barbara, *J. Phys. Chem.* **1995**, *99*, 2016–2023; b) A. Hoermann, W. Jarzeba, P. F. Barbara, *J. Phys. Chem.* **1995**, *99*, 2006–2015; c) W. Jarzeba, *J. Mol. Liq.* **1996**, *68*, 1–11.

[15] a) A. E. Johnson, N. E. Levinger, P. F. Barbara, *J. Phys. Chem.* **1992**, *96*, 7841–7844; b) D. A. V. Kliner, J. C. Alfano, P. F. Barbara, *J. Chem. Phys.* **1993**, *98*, 5375–5389; c) P. K. Walhout, J. C. Alfano, K. A. M. Thakur, P. F. Barbara, *J. Phys. Chem.* **1995**, *99*, 7568–7580.

[16] E. Gershgoren, U. Banin, S. Ruhman, *J. Phys. Chem. A* **1998**, *102*, 9–16.

[17] P. K. Walhout, C. Silva, P. F. Barbara, *J. Phys. Chem.* **1996**, *100*, 5188–5199.

[18] a) N. Pugliano, D. K. Palit, A. Z. Szarka, R. M. Hochstrasser, *J. Chem. Phys.* **1993**, *99*, 7273–7276; b) N. Pugliano, A. Z. Szarka, S. Gnanakaran, M. Treichel, R. M. Hochstrasser, *J. Chem. Phys.* **1995**, *103*, 6498–6511; c) N. Pugliano, A. Z. Szarka, R. M. Hochstrasser, *J. Chem. Phys.* **1996**, *104*, 5062–5079; d) M. Volk, S. Gnanakaran, E. Gooding, Y. Kholodenko, N. Pugliano, R. M. Hochstrasser, *J. Phys. Chem. A* **1997**, *101*, 638–643.

[19] T.-K. Ha, H.-U. Gremlich, R. E. Bühler, *Chem. Phys. Lett.* **1979**, *65*, 16–18.

[20] R. Mehnert, O. Brede, J. Bos, W. Naumann, *Ber. Bunsen-Ges.* **1979**, *83*, 992–996.

[21] R. E. Bühler, B. Hurni, *Helv. Chim. Acta* **1978**, *61*, 90–96.

[22] H.-U. Gremlich, T.-K. Ha, G. Zumofen, R. E. Bühler, *J. Phys. Chem.* **1981**, *85*, 1336–1340.

[23] H. Miyasaka, H. Masuhara, N. Mataga, *Chem. Phys. Lett.* **1985**, *118*, 459–463.

[24] O. Brede, J. Boes, R. Mehnert, *Ber. Bunsen-Ges.* **1980**, *84*, 63–68.

[25] R. E. Bühler, *Radiat. Phys. Chem.* **1983**, *21*, 139–146, and references therein.

[26] a) J. P. Simons, P. E. R. Tatham, *J. Chem. Soc. A* **1966**, 854–859; b) G. P. Brown, J. P. Simons, *Trans. Faraday Soc.* **1969**, *65*, 3245–3257; c) P. Cadman, J. P. Simons, *Trans. Faraday Soc.* **1966**, *62*, 631–641; d) J. P. Simons, J. Yarwood, *Trans. Faraday Soc.* **1963**, *59*, 90–100.

[27] a) H. Mohan, K. N. Rao, R. M. Iyer, *Radiat. Phys. Chem.* **1984**, *23*, 505–508; b) H. Mohan, R. M. Iyer, *Radiat. Eff.* **1978**, *39*, 97–101.

[28] a) G. Maier, H. P. Reisenauer, J. Hu, L. J. Schaad, B. A. Hess, Jr., *J. Am. Chem. Soc.* **1990**, *112*, 5117–5122; b) G. Maier, H. P. Reisenauer, *Angew. Chem.* **1986**, *98*, 829–831; *Angew. Chem. Int. Ed. Engl.* **1986**, *25*, 819–823.

[29] L. Andrews, F. T. Prochaska, B. S. Ault, *J. Am. Chem. Soc.* **1979**, *101*, 9–15.

[30] H. Mohan, P. N. Moorthy, *J. Chem. Soc. Perkin Trans. 2* **1990**, 277–282.

[31] J. P. Simons, M. Dantus, *Faraday Discuss.* **1997**, *108*, 92–93.

[32] M. N. Glukhovtsev, R. D. Bach, *Chem. Phys. Lett.* **1997**, *269*, 145–150.

[33] A. E. Orel, O. Kühn, *Chem. Phys. Lett.* **1999**, *304*, 285–292.

[34] B. J. Schwartz, J. C. King, J. Z. Zhang, C. B. Harris, *Chem. Phys. Lett.* **1993**, *203*, 503–508.

[35] a) K. Saitow, Y. Naitoh, K. Tominaga, K. Yoshihara, *Chem. Phys. Lett.* **1996**, *262*, 621–626; b) Y. Naitoh, K. Saitow, K. Yoshihara, *Springer Series in Chemical Physics, Ultrafast Phenomena XI*, *Vol. 63*, Springer, New York, **1998**, pp. 624–626.

[36] A. N. Tarnovsky, J.-L. Alvarez, A. P. Yartsev, V. Sundström, E. Åkesson, *Chem. Phys. Lett.* **1999**, *312*, 121–130.

[37] a) W. M. Kwok, D. L. Phillips, *J. Chem. Phys.* **1996**, *104*, 2529–2540; b) X. Zheng, D. L. Phillips, *J. Phys. Chem. A* **2000**, *104*, 6880–6886; c) W. M. Kwok, C. Ma, A. W. Parker, D. Phillips, M. Towrie, P. Matousek, D. L. Phillips, *J. Chem. Phys.* **2000**, *113*, 7471–7478; d) Y. Li, D. L. Phillips, *Chem. Phys. Lett.* **2001**, *349*, 291–298.

[38] A. N. Tarnovsky, V. Sundström, E. Åkesson, T. Pascher, *J. Phys. Chem. A* **2004**, *108*, 237–249.

[39] T. Lenzer, K. Oum, J. Schroeder, K. Sekiguchi, *J. Phys. Chem. A* **2005**, *109*, 10824–10831.

[40] C. Grimm, A. Kandratsenka, P. Wagener, J. Zerbs, J. Schroeder, *J. Phys. Chem. A* **2006**, *110*, 3320–3329.

[41] J. Davidsson, J. Poulsen, M. Cammarata, P. Georgiou, R. Wouts, G. Katona, F. Jacobson, A. Plech, M. Wulff, G. Nyman, R. Neutze, *Phys. Rev. Lett.* **2005**, *94*, 245503/1–4.

[42] H. Mohan, K.-D. Asmus, *J. Chem. Soc. Perkin Trans. 2* **1987**, 1795–1800.

[43] a) J. P. Mittal, W. H. Hamill, *J. Am. Chem. Soc.* **1967**, *89*, 5749–5753, and references therein; b) E. P. Bertin, W. H. Hamill, *J. Am. Chem. Soc.* **1967**, *86*, 1301–1304.

[44] a) R. F. C. Claridge, J. E. Willard, *J. Am. Chem. Soc.* **1967**, *89*, 510–516, and references therein; b) R. M. Iyer, J. E. Willard, *J. Am. Chem. Soc.* **1966**, *88*, 4561–4564.

[45] G. Schmitt, F. J. Comes, *J. Photochem.* **1980**, *14*, 107–123.

[46] T. F. Hunter , K. S. Kristjansson, *Chem. Phys. Lett.* **1982**, *90*, 35–40.

[47] W. H. Pence, S. L. Baughcum, S. R. Leone, *J. Phys. Chem.* **1981**, *85*, 3844–3851.

[48] a) S. L. Baughcum, S. R. Leone, *J. Chem. Phys.* **1980**, *72*, 6531–6545; b) J. B. Koffend, S. R. Leone, *Chem. Phys. Lett.* **1981**, *81*, 136–141.

[49] M. Kawasaki, S. J. Lee, R. Bersohn, *J. Chem. Phys.* **1975**, *63*, 809–814.

[50] P. M. Kroger, P. C. Demou, S. J. Riley, *J. Chem. Phys.* **1976**, *65*, 1823–1834.

[51] K.-W. Jung, T. S. Ahmadji, M. A. El-Sayed, *Bull. Korean Chem. Soc.* **1997**, *18*, 1274–1280.

[52] J. Zhang, D. G. Imre, *J. Chem. Phys.* **1988**, *89*, 309–313.

[53] a) M. Braun, A. Materny, M. Schmitt, W. Kiefer, V. Engel, *Chem. Phys. Lett.* **1998**, *284*, 39–46; b) F. Duschek, M. Schmitt, P. Vogt, A. Materny, W. Kiefer, *J. Raman Spectrosc.* **1997**, *28*, 445–453.

[54] J. Zhang, E. J. Heller, D. G. Imre, D. Tannor, *J. Chem. Phys.* **1988**, *89*, 3602–3611.

[55] G. Barinovs, N. Markovic, G. Nyman, *J. Chem. Phys.* **1999**, *111*, 6705–6711.

[56] J. Sehested, T. Ellermann, O. J. Nielsen, *Int. J. Chem. Kinet.* **1994**, *26*, 259–272.

[57] K. Kimura, S. Nagakura, *Spectrochim. Acta* **1961**, *17*, 166–183.

[58] M. Ito, P. C. Huang, E. M. Kosower, *Trans. Faraday Soc.* **1961**, *57*, 1662–1673.

[59] In hexane, a coherent artifact was observed at the vicinity of $t=0$. The time constants of the fast-rise and decay components were ob-

tained by subtracting the artifact of neat solvent from the solution data. This phenomenon has never been observed in acetonitrile in the present and previous studies.[35, 77]

[60] The photolyzed solution for the recording of the difference spectrum was prepared by irradiating at 268 nm the sample solution in a quartz cell with a thickness of 1 mm in 5 min.

[61] W. Gabes, D. J. Stufkens, *Spectrochim. Acta Part A* **1974**, *30*, 1835–1841.

[62] A. I. Popov, *Halogen Chemistry, Vol. 1* (Ed.: V. Gutmann), Academic Press, New York, **1967**.

[63] a) W. Kiefer, H. J. Bernstein, *Chem. Phys. Lett.* **1972**, *16*, 5–9; b) K. Kaya, N. Mikami, Y. Udagawa, M. Mitsuo, *Chem. Phys. Lett.* **1972**, *16*, 151–153.

[64] G. Moser, A. Asenbaum, G. Doge, *J. Chem. Phys.* **1993**, *99*, 9389–9393.

[65] R. E. Bühler, *J. Phys. Chem.* **1972**, *76*, 3220–3228.

[66] a) R. L. Strong, J. A. Kaye, *J. Am. Chem. Soc.* **1976**, *98*, 5460–5464; b) R. L. Strong, F. J. Venditti, Jr., *Chem. Phys. Lett.* **1977**, *46*, 546–550.

[67] The free-energy gap ΔG before and after electron transfer was estimated by the following equation:[69] $\Delta G = I_p - E_A + P_+ + P_- - E_{int}$, in which I_p is the ionization potential of the donor (CH$_2$I$_2$: 9.52 eV), E_A is the electron affinity of the acceptor (I atom: 3.1 eV), P_+ and P_- are the polarization energies (CH$_2$I$_2^+$: −2.7 eV; I$^-$: −3.5 eV) obtained from reference [68], and E_{int} is the sum of the internal energies of CH$_2$I$_2$ and fragment I or I*. The internal energy of fragment I or I* was estimated from the sum of the translational energy of the recoiling fragment I or I* after photodissociation by referring to values from references [50] and [51] and the energy of the spin-excited state of I*.

[68] I. Messing, J. Jortner, *Chem. Phys.* **1977**, *24*, 183–189.

[69] R. A. Marcus, *J. Chem. Phys.* **1956**, *24*, 966–978.

[70] J. L. Gebicki, A. S. Domazou, T.-K. Ha, G. Cirelli, R. E. Bühler, *J. Phys. Chem.* **1994**, *98*, 9570–9576.

[71] J. T. Hynes, R. Kapral, G. M. Torrie, *J. Chem. Phys.* **1980**, *72*, 177–188.

[72] J. N. Israelachvili, *Intermolecular and Surface Forces*, Academic Press, New York, **1985**.

[73] J. J. Jasper, *J. Phys. Chem. Ref. Data* **1972**, *1*, 841–1009.

[74] Due to its largest surface energy among molecular liquids, neat liquid CH$_2$I$_2$ is the most popular system for measuring the contact angle of a liquid droplet on solid surfaces.

[75] A. S. Carson, P. G. Laye, J. B. Pedley, A. M. Welsby, J. S. Chickos, S. Hosseini, *J. Chem. Thermodyn.* **1994**, *26*, 1103–1109.

[76] J. I. Steinfeld, J. S. Francisco, W. L. Hase, *Chemical Kinetics and Dynamics*, Prentice Hall, New Jersey, **1989**.

[77] a) K. Ohta, Y. Naitoh, K. Saitow, K. Tominaga, N. Hirota, K. Yoshihara, *Chem. Phys. Lett.* **1996**, *256*, 629–634; b) K. Ohta, Y. Naitoh, K. Tominaga, N. Hirota, K. Yoshihara, *J. Phys. Chem. A* **1998**, *102*, 35–44; c) K. Ohta, Y. Naitoh, K. Tominaga, K. Yoshihara, *J. Phys. Chem. A* **2001**, *105*, 3973–3980.

[78] Y. Inokuchi, Y. Naitoh, K. Ohashi, K. Saitow, K. Yoshihara, N. Nishi, *Chem. Phys. Lett.* **1997**, *269*, 298–304.

[79] a) K. Saitow, K. Endo, R. Katoh, M. Kotani, *Chem. Phys. Lett.* **1994**, *229*, 323–327; b) K. Saitow, R. Matsumura, R. Katoh, M. Kotani, *Mol. Cryst. Liq. Cryst.* **1996**, *277*, 125–133.